6636 *Inorg. Chem.* **2010**, *49*, 6636–6645
DOI: 10.1021/ic1005709

Inorganic Chemistry
Article

Sequence-Specific Ni(II)-Dependent Peptide Bond Hydrolysis for Protein Engineering: Reaction Conditions and Molecular Mechanism

Edyta Kopera,[†] Artur Krężel,[‡] Anna Maria Protas,[†] Agnieszka Belczyk,[†] Arkadiusz Bonna,[†] Aleksandra Wysłouch-Cieszyńska,[†] Jarosław Poznański,[†] and Wojciech Bal*[,†,§]

[†]*Institute of Biochemistry and Biophysics, Polish Academy of Sciences, Pawińskiego 5a, 02-106 Warsaw, Poland,* [‡]*Laboratory of Protein Engineering, Faculty of Biotechnology, University of Wrocław, Tamka 2, 50-137 Wrocław, Poland, and* [§]*Central Institute for Labour Protection—National Research Institute, Czerniakowska 16, 00-701 Warsaw, Poland*

Received March 26, 2010

Recently we screened a combinatorial library of R_1-(Ser/Thr)-Xaa-His-Zaa-R_2 peptides (Xaa = 17 common α-amino acids, except Asp, Glu, and Cys; Zaa =19 common α-amino acids, except Cys; R_1 = CH_3CO-Gly-Ala, R_2 = Lys-Phe-Leu-NH_2) and established criteria for selecting Ser/Thr, Xaa, and Zaa substitutions optimal for specific R_1-Ser/Thr peptide bond hydrolysis in the presence of Ni(II) ions (Krężel, A.; Kopera, E.; Protas, A. M.; Poznański, J.; Wysouch-Cieszyńska, A.; Bal, W. *J. Am. Chem. Soc.* **2010**, *132*, 3355−3366). The screening results were confirmed by kinetic studies of hydrolysis of seven peptides: R_1-Ser-Arg-His-Trp-R_2, R_1-Ser-Lys-His-Trp-R_2, R_1-Ser-Ala-His-Trp-R_2, R_1-Ser-Arg-His-Ala-R_2, R_1-Ser-Gly-His-Ala-R_2, R_1-Thr-Arg-His-Trp-R_2, and R_1-Thr-His-His-Trp-R_2. In this paper, we used the same seven peptides to investigate the molecular mechanism of the hydrolysis reaction. We studied temperature dependence of the reaction rate at temperatures between 24 and 75 °C, measured stability constants of Ni(II) complexes with hydrolysis substrates and products, and studied the course of R_1-Ser-Arg-His-Trp-R_2 peptide hydrolysis under a broad range of conditions. We established that the specific square planar complex containing the Ni(II) ion bonded to the His imidazole nitrogen and three preceding peptide bond nitrogens (4N complex) is required for the reaction to occur. The reaction mechanism includes the N−O acyl shift, yielding an intermediate ester of R_1 with the Ser/Thr hydroxyl group. This ester hydrolyzes spontaneously, yielding final products. The Ni(II) ion activates the R_1−Ser peptide bond by destabilizing it directly through peptide nitrogen coordination and, indirectly, by imposing a strain in the peptide chain.

Introduction

There is ongoing interest in new methods of sequence-specific cleavage of the peptide bond. Previously, we found that peptides possessing a general sequence R_N-(Ser/Thr)-Xaa-His-Zaa-R_C, where Xaa = Ala or His, Zaa = Lys, and R_N and R_C = nonspecific N-terminal and C-terminal peptide sequences, undergo a specific hydrolysis of the R_N-(Ser/Thr) peptide bond in the presence of Ni(II) ions above a pH of 7, with an acceleration at a pH of 9−10.[1−4] The pH profile of hydrolysis of the CH_3CO-Thr-Glu-Thr-His-His-Lys-NH_2 peptide suggested that the reaction in question occurred specifically in a square-planar Ni(II) complex of this peptide.[4] Several-fold differences among reaction rates of individual peptides suggested that a systematic search might yield highly reactive substitutions in positions Xaa and Zaa.[2,4] If successful, this search could lead to a chemical endopeptidase system with a sequence specificity high enough for practical applications in protein engineering. For this purpose, we synthesized a combinatorial library of R_1-(Ser/Thr)-Xaa-His-Zaa-R_2 peptides, where Xaa residues included 17 common α-amino acids (except Asp, Glu, and Cys), Zaa residues included 19 common α-amino acids (except Cys), R_1 was CH_3CO-Gly-Ala, and R_2 was Lys-Phe-Leu-NH_2. We measured the Ni(II)-related hydrolysis of this library using MALDI-TOF mass spectrometry and performed a thorough statistical analysis of the relation between the reaction rate and the peptide sequence.[5] We found that bulky and hydrophobic residues were preferred in positions Xaa and Zaa. The Ser residue following the R_1 moiety yielded a higher number of active

*Author to whom correspondence should be addressed. Phone: +48 22 592 2346. Fax: +48 22 659 4636. E-mail: wbal@ibb.waw.pl.

(1) Bal, W.; Lukszo, J.; Białkowski, K.; Kasprzak, K. S. *Chem. Res. Toxicol.* **1998**, *11*, 1014–1023.
(2) Bal, W.; Liang, R.; Lukszo, J.; Lee, S.-H.; Dizdaroglu, M.; Kasprzak, K. S. *Chem. Res. Toxicol.* **2000**, *13*, 616–624.
(3) Mylonas, M.; Krężel, A.; Plakatouras, J. C.; Hadjiliadis, N.; Bal, W. *J. Chem. Soc., Dalton Trans.* **2002**, 4296–4306.
(4) Krężel, A.; Mylonas, M.; Kopera, E.; Bal, W. *Acta Biochim. Polon.* **2006**, *53*, 721–727.
(5) Krężel, A.; Kopera, E.; Protas, A. M.; Wysłouch-Cieszyńska, A.; Poznański, J.; Bal, W. *J. Am. Chem. Soc.* **2010**, *132*, 3355–3366.

Published on Web 06/15/2010

Table 1. Logarithmic Protonation Constants for Peptides Determined at 25 °C and I = 0.1 M (KNO_3)[a]

peptide	HL	H_2L	H_3L	H_4L
R_1-SRHW-R_2	9.81(1)	15.84(1)		
R_1-SKHW-R_2	10.88(3)	20.53(2)	26.57(3)	
R_1-SAHW-R_2	10.46(4)	16.89(5)		
R_1-SRHA-R_2	10.00(3)	16.38(3)		
R_1-SGHA-R_2	10.06(2)	16.56(4)		
R_1-TRHW-R_2	9.86(1)	15.91(1)		
R_1-THHW-R_2	9.89(1)	16.59(2)	22.49(3)	
SRHW-R_2	9.95(1)	16.83(1)	22.63(1)	
SKHW-R_2	10.36(2)	19.77(2)	26.51(2)	32.35(2)
SAHW-R_2	9.90(4)	16.89(1)	22.85(1)	
SRHA-R_2	10.04(3)	17.19(2)	23.22(2)	
SGHA-R_2	10.05(4)	17.45(4)	23.54(2)	
TRHW-R_2	10.02(1)	16.88(1)	22.72(1)	
THHW-R_2	9.91(2)	17.12(3)	23.32(3)	28.92(3)

[a] Standard deviations on the least significant digits, provided by SUPERQUAD are given in parentheses.[7]

peptides than the Thr residue in this position. On the basis of these results, we selected seven R_1-(Ser/Thr)-Xaa-His-Zaa-R_2 peptides (Table 1) and used them to confirm the library screening results with an accurate HPLC-based assay.[5] High enhancements of reaction rates for the most active peptides encouraged further studies. In this paper, we present a detailed analysis of the nickel(II) binding and hydrolysis process for those seven peptides. We used potentiometry combined with absorption spectroscopy as a method of choice to characterize Ni(II) binding to these peptides quantitatively in a broad pH range; studied the kinetics of hydrolysis under various pH's, temperatures, and reactant ratio conditions; and used FT-IR to demonstrate the intermediate reaction product. As a result, we propose a multistep mechanism of the hydrolysis reaction.

Experimental Section

Peptide Synthesis. The seven R_1-(Ser/Thr)-Xaa-His-Zaa-R_2 peptides presented in Table 1 were synthesized using the Fmoc strategy and purified as described in a recent paper.[5] (Ser/Thr)-Xaa-His-Zaa-R_2 peptides, also listed in Table 1, were obtained by overnight incubations of respective R_1-(Ser/Thr)-Xaa-His-Zaa-R_2 peptides at 45 °C and a pH of 10 in the presence of a high Ni(II) excess, followed by purification using HPLC and identification using ESI-MS (Q-Tof1) as described before.[5]

Potentiometry. Potentiometric titrations were performed on a MOLSPIN automatic titrator, using InLab 422 combined glass-Ag/AgCl electrodes (Mettler-Toledo), which were calibrated daily by nitric acid titrations.[6] A 0.1 M NaOH (carbon dioxide free) was used as titrant. Sample volumes of 1.5−2 mL were used. The samples contained 0.5 mM peptides, dissolved in 4 mM HNO_3/96 mM KNO_3. The Ni(II) complex formation was studied using a 5−10% excess of peptides over Ni(II). The pH range for all potentiometric experiments was from 2.7 to 11.6. All experiments were performed under argon at 25 °C. The data were analyzed using the SUPERQUAD program.[7] Additional calculations were performed using the HYPERQUAD suite.[8] Three to five titrations were included simultaneously into calculations, separately for protonation and Ni(II) complexation.

UV−vis Spectroscopy. The spectra were recorded at 25 °C on a Cary 50-Bio (Varian) UV−vis spectrometer over the spectral range of 300−1100 nm, with samples containing 0.95 mM peptide and a metal-to-peptide ratio of 1:1.05, using a 1 cm cuvette. The samples were titrated with NaOH in the pH range of 2.4−11.6, by careful manual additions of very small amounts of the concentrated base solution.

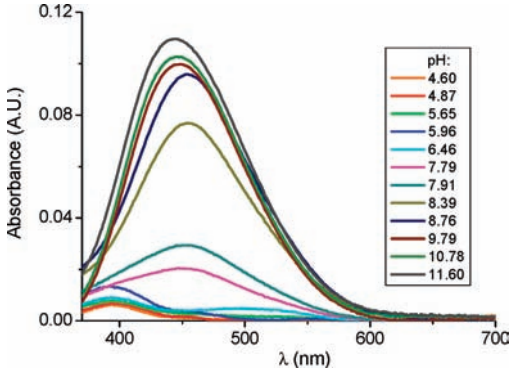

Figure 1. Selected UV−vis spectra of complexes formed by the R_1-SRHW-R_2 peptide (0.95 mM) with Ni(II) ions (0.9 mM). The pH values are indicated in the graph.

HPLC Measurements of Hydrolysis Rates. The temperature dependence of hydrolysis rates was studied for peptides presented in Table 1 at 24, 30, 37, 45, 55, 60, 68, and 75 °C. The samples, incubated in a water bath at temperatures controlled within ±0.5 °C, contained 1 mM peptide and 1.2 mM Ni(II) in a 20 mM Tris buffer at a pH of 8.2 or in a mixed PTB buffer (40 mM phosphate, 20 mM Tris, and 20 mM borax) at a pH of 11.6. Control runs were performed under identical conditions, in the absence of Ni(II) ions. The variable pH study of the hydrolysis of 1 mM R_1-Ser-Arg-His-Trp-R_2 peptide in the presence of 1.2 mM Ni(II) was also done using mixed PTB buffers set at various pH values, at 25 °C. In a further experiment, 1 mM R_1-Ser-Arg-His-Trp-R_2 peptide was incubated in a 20 mM Hepes buffer, at a pH of 8.2, in the presence of Ni(II) concentrations of 0.5, 0.75, 1.2, 2, 3, 4, 5, and 7 mM at 45 °C. The effects of phosphate, Tris, and Hepes buffers were also studied at a pH of 8.2 and 45 °C, using 20 mM buffer concentrations. In all cases, 20 μL aliquots of incubated samples were periodically removed from the reaction mixtures. An excess of 5% (v/v) TFA in water was added in order to stop the hydrolysis reaction. These samples were stored at 4 °C before injection into the HPLC system (Breeze, Waters) equipped with an autosampler and a double wavelength detector, set to 220 and 280 nm. An analytical C18 column (ACE, 250 × 4.6 mm) was used. The eluting solvent A was 0.1% (v/v) TFA in water, and solvent B was 0.1% (v/v) TFA in 90% (v/v) acetonitrile. In a typical analysis, 20 μL of each sample containing TFA was diluted in 180 μL of water and placed in a glass insert in the autosampler carousel. A total of 150 μL of such a sample was injected automatically into the HPLC system. The substrate and hydrolysis products were separated in a linear gradient of 10−40% B over 15 min, followed by 10 min of isocratic elution at 40% B, at the flow rate of 1 mL/min. The peaks were identified on a Q-Tof1 ESI-MS instrument. Pseudo-first-order kinetic constants were calculated using Microcal Origin, v. 8.0 (OriginLab).

Solid State Sample Preparation and FT-IR Spectroscopy. In order to ensure the maximum homogeneity and reproducibility of measurements, the samples of reaction substrates (R_1-Ser-Arg-His-Trp-R_2 and R_1-Thr-Arg-His-Trp-R_2), final products (Ser-Arg-His-Trp-R_2 and Thr-Arg-His-Trp-R_2), and corresponding intermediate products were prepared in the course of a controlled hydrolysis reaction of 10 mM peptides in the presence of equimolar $Ni(NO_3)_2$, in a 20 mM Tris buffer, at a pH of 8.2 and at 50 °C, followed by multiple HPLC separations on a Waters 600 system, using an ACE C18 analytical column. The pooled fractions of reaction substrates and final products

(6) Irving, H.; Miles, M. G.; Pettit, L. D. *Anal. Chim. Acta* **1967**, *38*, 475–488.
(7) Gans, P.; Sabatini, A.; Vacca, A. *J. Chem. Soc., Dalton Trans.* **1985**, 1195–1199.
(8) Gans, P.; Sabatini, A.; Vacca, A. *Talanta* **1996**, *43*, 1739–1753.

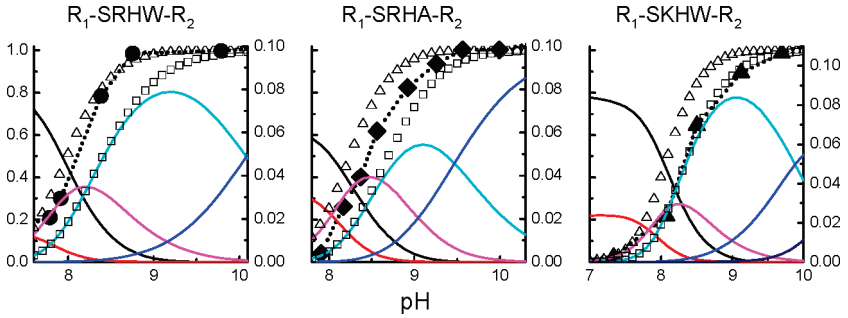

Figure 2. Partial species distribution diagrams for Ni(II) complex of selected R_1-(S/T)XHZ-R_2 peptides at 25 °C, calculated for concentrations used in UV−vis spectroscopy (0.9−1.0 mM peptides, 5% excess of peptides over Ni(II) ions) using stability constants provided in Tables 2 and 3. The common scale left-side axes represent molar fractions of Ni(II) complexes. Individual complex types are color-marked as follows: black, Ni(II) aqua ion; red, 1N complex; magenta, 3N complex; cyan, blue, and navy, 4N complexes undergoing stepwise deprotonations. Open triangles mark the sum of 3N and 4N complexes; open squares mark the sum of 4N complexes only. The variable scale right-side axes provides absorbances at the d−d band maximum of low-spin complexes (Table 4), marked with solid symbols. (See Supporting Information Figure S1 for full species distribution diagrams and Supporting Information Figure S2 for comparison plots for all seven peptides). Error bars were omitted for clarity, as they were smaller than the symbols in all cases.

Table 2. Logarithmic Ni(II) Complex Formation Constants for Peptides Determined at 25 °C and I = 0.1 M (KNO_3)[a]

peptide	NiH_3L	NiH_2L	NiHL	NiL	$NiH_{-1}L$	$NiH_{-2}L$	$NiH_{-3}L$
R_1-SRHW-R_2	n.d.	n.d.	12.2(2)	n.d.	−2.98(5)	−11.50(5)	−21.30(4)
R_1-SKHW-R_2	n.d.	23.15(6)	n.d.	7.5(3)	−0.61(1)	−10.49(3)	−21.18(3)
R_1-SAHW-R_2	n.d.	n.d.	13.70(3)	n.d.	−2.55(2)	−11.22(2)	−22.11(3)
R_1-SRHA-R_2	n.d.	n.d.	12.9(1)	n.d.	−3.12(6)	−11.74(4)	−21.21(5)
R_1-SGHA-R_2	n.d.	n.d.	12.97(6)	n.d.	−3.26(5)	−11.36(3)	−21.15(3)
R_1-TRHW-R_2	n.d.	n.d.	13.17(4)	n.d.	−2.98(6)	−12.08(6)	−22.19(7)
R_1-THHW-R_2	n.d.	19.1(1)	13.23(3)	n.d.	−2.63(2)	−11.37(2)	−21.74(2)
SRHW-R_2	n.d.	20.4(1)	n.d.	n.d.	1.67(4)	n.c.	n.c.
SKHW-R_2	30.2(2)	23.8(1)	n.d.	10.87(6)	0.93(3)	n.c.	n.c.
SAHW-R_2	n.d.	20.86(5)	n.d.	8.16(8)	2.286(3)	n.c.	n.c.
SRHA-R_2	n.d.	20.4(1)	n.d.	8.05(4)	−1.36(7)	n.c.	n.c.
SGHA-R_2	n.d.	n.d.	n.d.	9.93(4)	1.66(6)	n.c.	n.c.
TRHW-R_2	n.d.	19.6(2)	n.d.	n.d.	1.34(3)	n.c.	n.c.
THHW-R_2	n.d.	16.3(1)	n.d.	5.7(5)	−0.95(6)	n.c.	n.c.

[a] Standard deviations on the least significant digits, provided by SUPERQUAD or HYPERQUAD, are given in parentheses.[7,8] Abbreviations: n.c., not calculated; n.d., not detected.

were concentrated on a rotary evaporator, followed by lyophilization. The identities and purities of lyophilized samples were controlled by HPLC and ESI-MS. The intermediate product fractions were lyophilized in 7 mL portions, omitting the rotary evaporator step. Each portion was controlled by ESI-MS. Amounts of ca. 4 mg of substrates, 2 mg of final products, and 1 mg of intermediate products were obtained. The purities of the latter were about 90%, with final products as main impurities.

The solid state FT-IR spectra were recorded at 25 °C on an Excalibur (Bio-Rad) Fourier-transform infrared spectrometer over a spectral range of 2000−1000 cm^{-1} in KBr pellets (Merck).

Results

Potentiometric and Spectrophotometric Study of Formation of Ni(II) Complexes. Table 1 presents protonation constants of all 14 peptides studied, seven R_1-(S/T)XHZ-R_2 hydrolysis substrates and seven corresponding (S/T)XHZ-R_2 products[5] (one letter amino acid codes are used for the sake of brevity, (S/T) denotes "Ser or Thr"). The assignments of individual protonation macroconstants to respective chemical groups, pK values above 9 to Lys amines, pK values around 7 in (S/T)XHZ-R_2 peptides to N-terminal amines, and pK values of 5.6−6.5 to His imidazoles, are based on previous studies of analogous peptides.[1−4,9−12]

At a weakly acidic pH, all R_1-(S/T)XHZ-R_2 peptides formed high-spin (octahedral) complexes which underwent spin pairing in neutral to alkaline solutions, yielding square-planar complexes.[12] This property is illustrated in Figure 1, which presents the UV−vis titration of the Ni(II)-[R_1-SRHW-R_2] system. Figure 2 provides the plots of pH dependence of Ni(II) complexes of selected R_1-(S/T)XHZ-R_2 peptides, calculated using stability constants, obtained by potentiometry (Table 2). These calculations were made for conditions used in UV−vis experiments, to enable direct comparison with the values of absorption at the d−d band maximum of the major square-planar species (A_{max}), overlaid on these plots. The corresponding λ_{max} and ε values are provided in Table 3. The set of four metal complexes (NiHL, $NiH_{-1}L$, $NiH_{-2}L$, and $NiH_{-3}L$) provided the best fit to experimental titration curves obtained for all of these peptides except R_1-SKHW-R_2 and R_1-THHW-R_2. (L in these formulas means a peptide devoid of all hydrogen ions which can dissociate upon the pH change without metal ion assistance, including those at imidazole rings and amine groups; the negative

(9) Bal, W.; Kozłowski, H.; Pettit, L. D.; Robbins, R. *Inorg. Chim. Acta* **1995**, *231*, 7–12.
(10) Bal, W.; Chmurny, G. N.; Hilton, B. D.; Sadler, P. J.; Tucker, A. *J. Am. Chem. Soc.* **1996**, *118*, 4727–4728.
(11) Bal, W.; Jeżowska-Bojczuk, M.; Kasprzak, K. S. *Chem. Res. Toxicol.* **1997**, *10*, 906–914.
(12) Kozłowski, H.; Bal, W.; Dyba, M.; Kowalik-Jankowska, T. *Coord. Chem. Rev.* **1999**, *184*, 319–346.

Table 3. Parameters of d−d Bands of the Least Deprotonated Square-Planar 4N Ni(II) Complexes of Substrate Peptides[a]

peptide sequence	λ_{max} (nm)	ε (M^{-1} cm^{-1})
R_1-SRHW-R_2	453	103
R_1-SKHW-R_2	442	116
R_1-SAHW-R_2	447	115
R_1-SRHA-R_2	446	109
R_1-SGHA-R_2	444	127
R_1-TRHW-R_2	444	137
R_1-THHW-R_2	440	211
CH_3CO-TESHHK-NH_2[b]	445	157
CH_3CO-TASHHK-NH_2[b]	450	150
CH_3CO-TESAHK-NH_2[b]	442	125
CH_3CO-TETHHK-NH_2[c]	453	96

[a] Errors of ε determinations were smaller than 1 M^{-1} cm^{-1}. [b] Ref 3. [c] Ref 4.

indexes in complex formulas are related to main chain amide protons, released by Ni(II) ions upon the formation of 3N and 4N complexes.)

The NiHL complex, formed above pH 4, contains the Ni(II) ion coordinated solely to an imidazole ring nitrogen (1N). At higher pH values around 8, two amide donors deprotonate cooperatively, yielding the $NiH_{-1}L$ complex with the metal ion coordinated to the imidazole and two amide nitrogens (3N).[12] The next species, $NiH_{-2}L$ forms upon the deprotonation of the third amide nitrogen. It contains the Ni(II) ion bonded by the imidazole nitrogen and three amide nitrogens (4N). The final $NiH_{-3}L$ complex forms upon Lys side chain amine deprotonation. This event does not affect the Ni(II) binding mode. The R_1-SKHW-R_2 and R_1-THHW-R_2 peptides contain an additional proton exchanging residue, Lys or His, respectively. Therefore, their 1N complexes have the NiH_2L stoichiometry.

This extra proton in the R_1-THHW-R_2 complex is present at the uncoordinated His residue. Its deprotonation around a pH of 6.1 yielded NiHL, another 1N complex, which released two protons cooperatively around a pH of 8, similarly to complexes of all H_2L peptides. The resulting $NiH_{-1}L$ 3N complex and the subsequent $NiH_{-2}L$ and $NiH_{-3}L$ 4N species are analogous to those described above.

A minor 3N complex, of NiL stoichiometry, was detected for R_1-SKHW-R_2. This complex readily released a proton, yielding a $NiH_{-1}L$ 4N complex, with both Lys residues protonated. Subsequent deprotonations of these residues, yielding $NiH_{-2}L$ and $NiH_{-3}L$ complexes, did not affect the Ni(II) binding, analogously to peptides containing a single Lys residue. General structures of NiHL, $NiH_{-1}L$, $NiH_{-2}L$, and $NiH_{-3}L$ complexes are presented in Chart 1.

The comparison of potentiometric species distributions with spectroscopic profiles of low-spin complexes, represented by absorption values at $\lambda_{max} \sim 440-450$ nm, indicated significant differences between individual peptides. For three of them, R_1-SRHW-R_2, R_1-SAHW-R_2, and R_1-TRHW-R_2, the spectroscopic profile of low-spin species coincided precisely with 3N complex formation. For R_1-SKHW-R_2, R_1-THHW-R_2, and R_1-SGHA-R_2, the low-spin species signatures corresponded to the 4N complex formation. The electronic absorption profile of the remaining R_1-SRHA-R_2 peptide was located between the 3N and 4N complex formation curves. Therefore, the 3N species of this peptide contain both high spin and low

Chart 1. Structures of Ni(II) Complex Species, Formed by R_1-(S/T)-XHZ-R_2 Peptides, except R_1-SKHW-R_2 and R_1-THHW-R_2 Peptides, Which Carry an Additional Positive Charge at a Lys/His Residue, Respectively (See Text)[a]

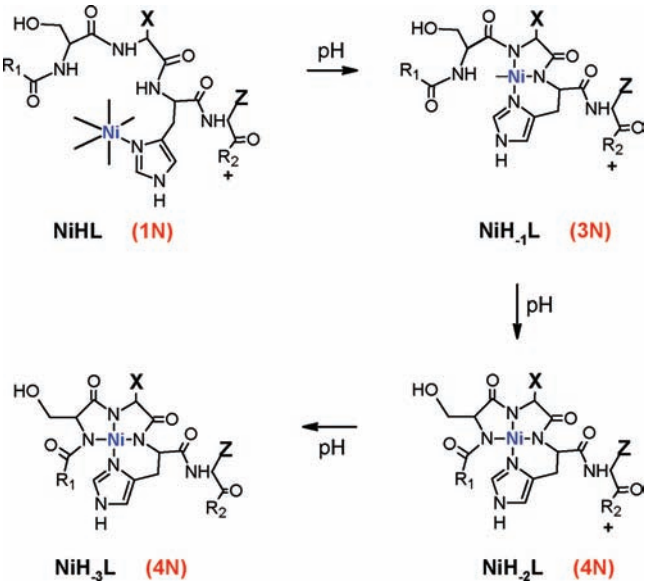

[a] The Ser analogs only are presented for clarity. Open bonds at the Ni(II) ion represent coordinated water molecules. The + sign at the R_2 moiety represents a positive charge of its Lys side chain.

spin isomers. The spin equilibria in Ni(II) peptide complexes depend on the number, space locations, and fine electronic properties of nitrogen ligands, and the transition point between the high and low spin states is typically located between the 3N and 4N coordinations. The variation observed among peptides studied is therefore due to details of peptide conformations in 3N complexes and does not affect the properties of 4N complexes. The full pH range species distribution plots are shown as Supporting Information Figure S1, and comparisons of spectroscopic and potentiometric profiles for all seven substrate peptides are provided as Supporting Information Figure S2. Figure 2 presents examples for each of three kinds of behavior: R_1-SRHW-R_2, R_1-SKHW-R_2, and R_1-SRHA-R_2. The d−d band parameters of the first (i.e., the least deprotonated) 4N complexes, presented in Table 3, are similar to analogous complexes of peptides susceptible to Ni(II) hydrolysis studied previously.

Stability constants of Ni(II) complexes with hydrolysis products were also measured. Only the C-terminal products were studied, because previous experiments demonstrated that Ni(II) ions remained complexed to them in the course of the hydrolysis process.[1−4] These constants are also provided in Table 2. The C-terminal reaction products contain a free S/T amine, and therefore they form stable square-planar 4N complexes at lower pH values than the substrates, already below pH 7.[1,10−12] Due to a very slow Ni(II) complexation reaction, the data points above pH 9 were considered unreliable and were not included in the calculations. As a result, the Lys deprotonations were not studied in these complexes. This limitation did not affect the data analysis presented below.

Detailed Studies of Conditions of Hydrolysis of the R_1-SRHW-R_2 Peptide. Our previous experiments indicated that the R_1-SRHW-R_2 peptide had the highest susceptibility

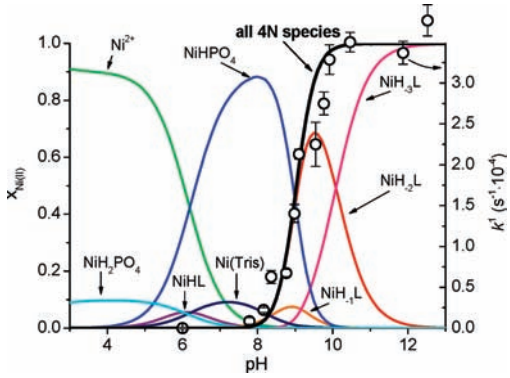

Figure 3. The pH dependence of the pseudo-first-order rate constant of the Ala−Ser peptide bond hydrolysis in 1 mM R_1-SRHW-R_2 peptide incubated with 1.2 mM $Ni(NO_3)_2$ in PTB buffers at 25 °C (circles), compared to the complex species distribution, calculated from data in Tables 2 and 3 and literature data on buffers.[13−15] The thick black line represents the sum of molar fractions of 4N complexes, $NiH_{-2}L$ and $NiH_{-3}L$.

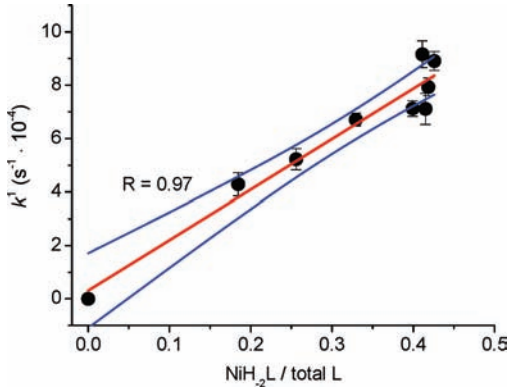

Figure 4. Linear relationship between the pseudo-first-order rate constant of the Ala−Ser peptide bond hydrolysis in the R_1-SRHW-R_2 peptide (1 mM) and the molar fraction of the $NiH_{-2}L$ complex of this peptide, relative to the total peptide pool. The experiments were performed at 45 °C in a 0.1 M Hepes buffer, at a pH of 8.2. The amounts of $NiH_{-2}L$ were calculated using stability data in Tables 2 and 3. The Ni(II) ion concentrations were added at concentrations between 0.25 and 7 mM. The trend line (red), 95% confidence bands (blue), and linear correlation coefficients R are marked in the plot.

to Ni(II)-related hydrolysis among all peptides tested.[5] Therefore, we chose this peptide for further studies of hydrolysis reaction conditions. First, the pH dependence of hydrolysis was investigated. The R_1-SRHW-R_2 peptide (1 mM) was incubated with Ni(II) ions (1.2 mM) in a series of PTB buffers with a pH between 6.0 and 12.5. HPLC was used to separate and quantitate reaction products, which were identified using ESI-MS. The reaction proceeded in two major steps, as indicated by the presence of the intermediate product, whose molecular mass and MS isotopic profile were identical with the substrate, but the HPLC retention time was different. In the preceding paper, the intermediate product peak was integrated together with the substrate peak in order to mimic the mass spectrometric library screening.[5] Here, we added the integral of the intermediate product peak, whenever it was detected to that of the final product. In this way, the kinetic data presented below corresponded to the first major step of the hydrolysis reaction. In full agreement with previous experiments, the final reaction products were the N-terminal R_1-OH dipeptide and the C-terminal (S/T)XHZ-R_2 peptide. This N-terminal product was not detected in HPLC as a separate peak, due to its low size. Thanks to its low absorption at 220 nm, its omission in HPLC peak integration did not bias the integration results significantly.[5] Figure 3 presents the pH dependence of the pseudo-first-order rate constant, compared with the species distribution of Ni(II)-[R_1-SRHW-R_2] complexes in PTB buffers. Protonation and stability constants of R_1-SRHW-R_2 (Tables 1 and 2) and literature stability constants for phosphate and Tris Ni(II) complexes were used for calculations.[13,14] The Hepes buffer does not bind Ni(II) ions at a pH of 7.4.[15] We found no indication of such binding at higher pH values either. Figure 3 demonstrates that a strict match between the rate of hydrolysis and the amount of the 4N Ni(II) complexes of the R_1-SRHW-R_2 peptide was seen.

Table 4. First-Order Rate Constants for Hydrolysis of R_1-SRHW-R_2 (1 mM) in the Presence of Ni(II) (1.2 mM) in 20 mM Tris, Hepes, and Phosphate Buffers at 45 °C and pH 8.2[a]

buffer	molar fraction of 4N complexes[b]	k^1 ($s^{-1} \times 10^{-5}$)	k^1 ($s^{-1} \times 10^{-4}$) (extrapolated)
Tris	0.2	4.9(6)	2.5(3)
Hepes	0.33	9(2)	2.8(6)
phosphate	0.033	0.74(9)	2.3(3)

[a] Extrapolation of these constants on the basis of the molar fraction of 4N complexes are shown for comparison. Standard deviations on the least significant digits are given in parentheses. [b] Calculated using literature stability constants for Ni(II) complexes with phosphate[12] and Tris.[13]

The effect of Ni(II) concentration on the rate of R_1-SRHW-R_2 hydrolysis at a constant pH was investigated next. Samples of 1 mM R_1-SRHW-R_2 were incubated in a Hepes buffer at a pH of 8.2 with Ni(II) ions at concentrations between 0.5 mM and 7 mM. Figure 4 presents the relationship between the hydrolysis rate and the calculated amounts of the $NiH_{-2}L$ complex. A very good linear correlation between these parameters was obtained (R = 0.97). Random deviations from the trend line were observed at higher Ni(II) concentrations and were likely due to partial precipitation of uncoordinated Ni(II) ions as hydroxide.

Finally, the effect of buffers on the rate of hydrolysis was studied at 45 °C as described above, separately in 20 mM Tris, Hepes, and sodium phosphate buffers, all at a pH of 8.2, for 1 mM peptide and 1.2 mM Ni(II). The results are presented in Table 4. Calculations using experimental rate constants, R_1-SRHW-R_2 stability constants presented above, and the literature data for buffers,[13,14] shown in Table 4, indicate that, indeed, the R_1-S peptide bond hydrolysis rate was dependent primarily on the amount of the 4N complex in solution at the beginning of incubation.

The Temperature Dependence of Hydrolysis Rates. The Ni(II)-dependent hydrolysis of peptides, presented in Table 1, was previously studied at 37 and 45 °C.[5] These peptides are studied here in a broad temperature range of 24 to 75 °C, in order to gain better insight into the

(13) Bal, W.; Lukszo, J.; Kasprzak, K. S. *Chem. Res. Toxicol.* **1996**, *9*, 435–440.
(14) Krężel, A.; Szczepanik, W.; Sokołowska, M.; Jeżowska-Bojczuk, M.; Bal, W. *Chem. Res. Toxicol.* **2003**, *16*, 855–864.
(15) Sokołowska, M.; Wszelaka-Rylik, M.; Poznański, J.; Bal, W. *J. Inorg. Biochem.* **2009**, *103*, 1005–1013.

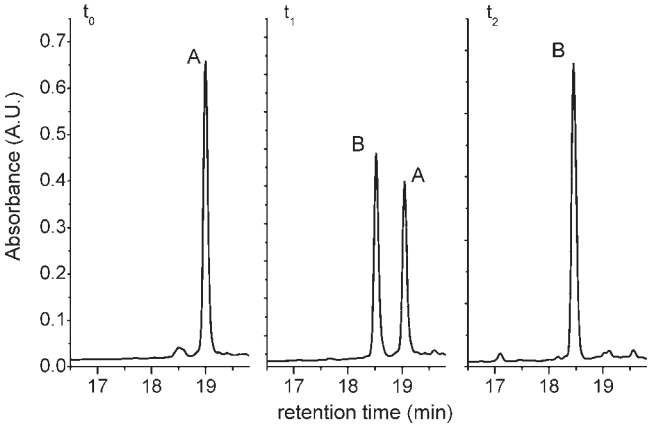

Figure 5. HPLC chromatograms of 1 mM R_1-SKHW-R_2 peptide incubated with 1.2 mM Ni(II) ions at 45 °C and a pH of 11.6 (PTB buffer), recorded at incubation times t_0 = 0 min (before incubation), t_1 = 12 min, and t_2 = 61 min. Peak labels: A, R_1-SKHW-R_2 reaction substrate; B, SKHW-R_2 reaction product.

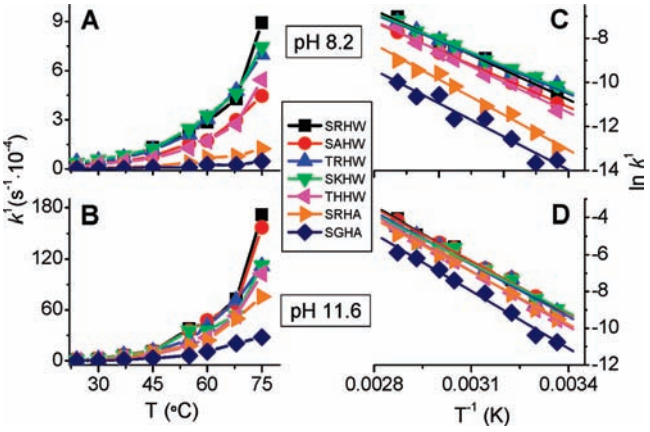

Figure 6. Temperature dependence of the pseudo-first-order rate constants of the R_1−Ser/Thr peptide bond hydrolysis and corresponding Arrhenius plots (eq 1A) for reactions in 20 mM Tris at a pH of 8.2 (top) and in PTB buffer at a pH of 11.6 (bottom). Straight lines represent linear fits of Arrhenius plot data for individual peptides. Error bars were omitted for clarity, as they were smaller than the symbols in all cases.

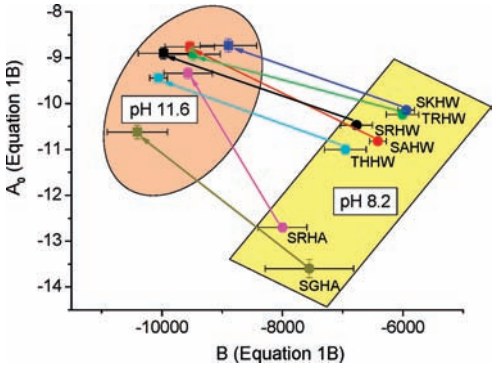

Figure 7. Clustering of hydrolytic susceptibilities of peptides. The plot parameters result from the fitting of hydrolysis rate constants (Supporting Information Tables 1 and 2, Figure 6C and D) to the modified Arrhenius function (eq 1B). Arrows illustrate the changes of parameters for individual peptides between a pH of 8.2 and 11.6.

reaction mechanism. The experiments were performed at two pH values. A highly selective pH value of 8.2 was used previously for library screening. The results of the preceding section indicate that the amount of the active 4N complex should be a major factor influencing the rate of hydrolysis at this pH value. At a pH of 11.6, on the other hand, all peptides studied formed solely 4N complexes (Table 2, Supporting Information Figure S1). Therefore, they were expected to exhibit maximal reaction rates at this high pH.

Typical analytical chromatograms for the reaction at a pH of 11.6 are shown in Figure 5. The intermediate reaction product (IP), seen at a pH of 8.2 previously,[5] was absent for all peptides and temperatures at a pH of 11.6.

Ni(II)-free control experiments at a pH of 8.2 and 11.6 demonstrated an absence of background hydrolysis of peptides studied, similarly to those presented previously for the same peptides at a pH of 8.2.[5] At longer incubation times at a pH of 11.6, a novel peak neighboring that of the substrate peak was detected in some Ni(II)-free samples (see Supporting Information Figure S3). This, however, was not a product of hydrolysis, because its mass was identical to that of the substrate and its retention time was significantly different from those of IPs and very similar to that of the reaction substrate. Such a product was never seen in the presence of Ni(II) ions. The unspecific hydrolysis of the peptides to single amino acids or dipeptides can also be excluded, because no loss of material could be noted in subsequent chromatograms.

The temperature dependence of pseudo-first-order rate constants (k^1) measured in these experiments is presented in Figure 6 (panels A and B). Corresponding numeric data are provided in Supporting InformationTables S1 and S2. As expected, the hydrolysis was much faster at a pH of 11.6 for all peptides. Arrhenius plots of kinetic data, fitted to the linear Arrhenius function (eq 1A), are shown in Figure 6 (panels C and D). In this form of the Arrhenius function, parameter A represents the extrapolation of ln k^1 to the infinite temperature. A modified function can also be used (eq 1B), with parameter A_0 representing the value of ln k^1 at 25 °C, calculated by interpolation over all experimental temperatures (the experiments were performed at 24, rather than 25 °C).

$$ln(k^1) = A + B \times T^{-1} \qquad (1A)$$

$$ln(k^1) = A_0 + B \times (T^{-1} - 298.15^{-1}) \qquad (1B)$$

Figure 7 presents a plot generated using eq 1B, which provides the means to cluster peptides studied according to their hydrolytic susceptibilities. Arrows mark the changes of parameters for individual peptides between a pH of 8.2 and a pH of 11.6. It has to be noted that parameter B, while related to activation energy, has no direct physical interpretation and is used purely as a means of peptide clustering.

The Intermediate Reaction Product. As mentioned above, HPLC analysis of the reaction mixtures revealed the presence of the intermediate reaction product (IP). Its molecular mass determined by ESI-MS was exactly the same as that of the substrate. The presence of IP was observed for all peptides incubated with Ni(II) ions at a pH of 8.2. Representative examples are shown in Figure 8. IP appeared usually at the beginning of the hydrolysis reaction and remained nearly to its end. It should be noticed that in most cases, samples were stored at 4 °C before the HPLC

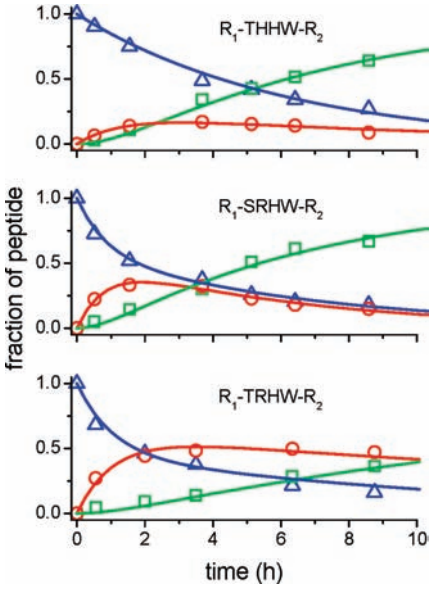

Figure 8. The relative amount of the intermediate hydrolysis product (circles), compared to those of the substrate (triangles) and product (squares), during the reaction at a pH of 8.2 (20 mM Tris) and a temperature of 45 °C, for peptides representing low (R_1-THHW-R_2, top), medium (R_1-SRHW-R_2, middle), and high (R_1-TRHW-R_2, bottom) levels of intermediate product. The lines represent fits to eqs 2 (red) and 3 (green). The blue lines were calculated by subtracting the red and green lines from the molar fraction of 1.

analysis for various amounts of time, required by sample pooling for overnight autosampler runs. The hydrolysis comes to a halt at these low temperatures, but we did not perform systematic studies of IP stability under these conditions, so the results shown in Figure 8 are not necessarily strictly quantitative. Nevertheless, they reveal reproducible and substantial differences of IP amounts between individual peptides. Despite the above reservations, we attempted a more thorough kinetic analysis of these data, using an explicit two-step model, S → IP → P, where the first and the second step are described by first-order rate constants k_1 and k_2. These constants are correlated with the amounts of the intermediate and final products by eq 2, used for the intermediate hydrolysis product IP fitting, and eq 3, used for the final hydrolysis product P fitting.

$$A = \frac{k_1 \cdot A_0}{k_2 \cdot k_1} \times (e^{-k_1 t} - e^{-k_2 t}) \qquad (2)$$

$$A = A_0 \cdot \left(1 + \frac{1}{k_1 - k_2}\right) \times k_2 \times e^{k_1 t} - k_1 \times e^{-k_2 t} \qquad (3)$$

In regard to both eqs 2 and 3, where A and A_0 denote the momentary and initial concentrations of a given species, respectively, the rates obtained for these three reactions are presented in Table 5.

The nature of the IPs was studied using FT-IR spectroscopy in KBr pellets. Figure 9 presents the 2000−1500 cm^{-1} regions of absorption mode IR spectra of substrates, IP, and final products of Ni(II)-dependent hydrolysis of R_1-SRHW-R_2 and R_1-TRHW-R_2 peptides, those two that yielded the highest amounts of intermediate products during hydrolysis. The IP spectra specifically exhibited an identical novel band at 1750 cm^{-1}, which is a characteristic position of a C=O stretching vibration in saturated esters.[16]

Table 5. Values of k_1 and k_2 First-Order Rate Constants, Obtained from the Fitting of Data Presented in Figure 8 (Hydrolysis at pH 8.2, 20 mM Tris, 45 °C) to Kinetic eqs 2 and 3[a]

peptide	k_1 ($s^{-1} \times 10^{-4}$)	k_2 ($s^{-1} \times 10^{-4}$)
R_1-THHW-R_2	2.2(5)	0.40(3)
R_1-SRHW-R_2	3.3(5)	0.46(7)
R_1-TRHW-R_2	2.7(5)	0.16(1)

[a] Standard deviations on the least significant digits are given in parentheses.

Discussion

Formation of 4N Complexes. The protonation-corrected stability constant $^*K$ is a facile tool for comparing stabilities of isostructural complexes with peptides carrying different numbers of protonating groups.[9,12,13] Such constants are presented in Table 6 for complexes of reaction substrates and products determined in this work (labeled $^*K_S$ and $^*K_P$, respectively, according to eqs 4, 4A, 5, and 5A)

$$\log {}^*K_S = \log \beta\{NiH_{-2}L\} - \log \beta\{H_2L\} \qquad (4)$$

for R_1-SKHW-R_2

$$\log {}^*K_S = (\log \beta\{NiH_{-1}L\} - \log \beta\{H_3L\} \qquad (4A)$$

$$\log {}^*K_P = \log \beta\{NiH_{-1}L\} - \log \beta\{H_3L\} \qquad (5)$$

for SKHW-R_2

$$\log {}^*K_P = \log \beta\{NiL\} - \log \beta\{H_4L\} \qquad (5A)$$

Log $^*K_S$ values are in the range of −27.05 (R_1-SRHW-R_2) to −28.12 (R_1-SRHA-R_2). This range is similar to that obtained previously for analogous complexes of acetyl-TE-(S/T)XHK-amide peptides (−27.26 to −28.58),[3,4] and for other, nonhydrolyzable peptides containing a His residue in the middle of their peptide chains, e.g., −28.70,[19] −28.16,[20] and −28.87.[21] Also, d−d band parameters (Table 3) are within the typical range of values for such complexes. No systematic relationships between these parameters and complex stabilities were found.

The analogous 4N complexes of reaction products are much stronger than those of reaction substrates. This is due to the presence of the amine, rather than amide

(16) Smith, B. C. *Infrared spectral interpretation: a systematic approach*, CRC Press LLC: Boca Raton, FL, 1999; p 109.
(17) Sokołowska, M.; Krężel, A.; Dyba, M.; Szewczuk, Z.; Bal, W. *Eur. J. Biochem.* **2002**, *269*, 1323–1331.
(18) Bal, W.; Dyba, M.; Kozłowski, H. *Acta Biochim. Polon.* **1997**, *44*, 467–476.
(19) Zoroddu, M. A.; Kowalik-Jankowska, T.; Kozłowski, H.; Molinari, H.; Salnikow, K.; Broday, L.; Costa, M. *Biochem. Biophys. Acta* **2000**, *1475*, 163–168.
(20) Zoroddu, M. A.; Kowalik-Jankowska, T.; Kozłowski, H.; Salnikow, K.; Costa, M *J. Inorg. Biochem.* **2001**, *95*, 47–54.
(21) Karavelas, T.; Mylonas, M.; Malandrinos, G.; Plakatouras, J. C.; Hadjiliadis, N.; Młynarz, P.; Kozłowski, H. *J. Inorg. Biochem.* **2005**, *99*, 606–615.

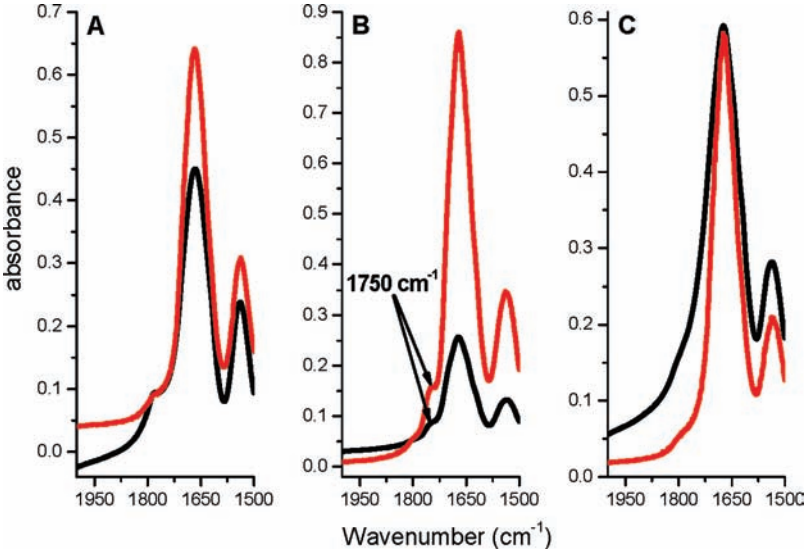

Figure 9. The 2000−1500 cm^{-1} regions of absorption mode IR spectra of substrates (A), IP (B), and final products (C) of Ni(II)-dependent hydrolysis of R_1-SRHW-R_2 (red) and R_1-TRHW-R_2 (black) peptides. The IP spectra (B) specifically exhibited a novel band at 1750 cm^{-1}, characteristic of a C═O stretching vibration in saturated esters (marked with arrows).

Table 6. Protonation-Corrected Stability Constants for 4N Ni(II) Complexes of Reaction Substrates and Products[a]

peptide	log $*K_S$	log $*K_P$	log $*K_P$ − log $*K_S$
R_1-SRHW-R_2	−27.05	−20.96	6.09
R_1-SKHW-R_2	−27.35	−21.80	5.55
R_1-SAHW-R_2	−28.11	−20.56	7.55
R_1-SRHA-R_2	−28.12	−24.58	3.54
R_1-SGHA-R_2	−27.92	−21.88	6.04
R_1-TRHW-R_2	−27.99	−21.38	6.74
R_1-THHW-R_2	−27.97	−23.22	4.75

[a] Log $*K_S$ and Log $*K_P$ are defined by eqs 4A and 4, respectively.

nitrogen at the S/T residue.[12] Interestingly, log $*K_P$ values presented in Table 6 exhibit a much broader variability, between −20.56 (SAHW-R_2) and −24.70 (SRHA-R_2). There is a large body of literature data on stabilities of complexes of such His-3 peptides. The generic sequence GGH is characterized with the log $*K_P$ value of −21.81,[22] while the tetrapeptide exhibiting a molecular crowding around the bound Ni(II) ion, VIHN, yielded a log $*K_P$ value of −19.75.[10] Even higher log $*K_P$ values were found for two human protamine peptides containing the basic Arg residue in the N-terminal position, −19.23 and −19.29.[11] Peptide models of the N-terminus of human serum albumin yielded log $*K_P$ values of −19.48 to −21.72.[17,23] The strongest complex of a His-3 peptide composed of standard amino acids, SSH-NH_2, exhibited a log $*K_P$ of −18.50.[23] Tetrapeptides SAHK-NH_2 and SHHK-NH_2 yielded log $*K_P$ values of −21.80 and −19.14, respectively.[24] Altogether, the Ni(II) complexes with hydrolysis products studied here exhibited moderate to low stabilities in their class of compounds.

Molecular Mechanism of Hydrolysis. The results of experiments presented in Figures 3 and 4 and in Table 4 demonstrated beyond a doubt that the hydrolysis of the Ala−Ser peptide bond in the R_1-SRHW-R_2 peptide occurred specifically in the 4N Ni(II) complex. The formation of just any low spin complex is not sufficient, because the 3N complex of this peptide, also low spin, is not susceptible to hydrolysis (see Figures 2 and 3). The hypothetical formation of a square-pyramidal low-spin Ni(II) complex, with an axial hydroxyl group that could act as a hydrolysis catalyst, while chemically plausible, can be ruled out. In such case, a significant pH dependence of the rate should be observed in the range of 100% formation of the 4N complex. This was not the case (see Figure 3, pH range above 10). Furthermore, such a species was not detected by potentiometry (Table 2). Also, the formation of such species would be hindered rather than enhanced by bulky X and Z substituents, which were shown to facilitate the hydrolysis.[5]

Figure 10 presents the predicted hydrolysis rate constants at pH 8.2 and 25 °C, calculated for all seven peptides studied using their rate constants at a pH of 11.6 (100% of 4N complex formation) multiplied by the relative concentration of the sum of their 4N species at a pH of 8.2 (calculated from potentiometric results). These predicted constants agree very well with experimental rate constants, actually measured at pH 8.2. The linear correlation of these values (red line) is not only strongly statistically significant ($p < 0.007$) but also agrees well with the ideal 1:1 relationship (dotted green line), which remains within the limit of 95% confidence bands of the correlation (blue curves). These relationships confirm that the hydrolysis occurs specifically in 4N complexes for all Ser and Thr peptides studied. Deviations from the ideal correlations are likely due to slight effects of the R_2 moiety Lys deprotonations on hydrolysis rates (see Figure 3 and Supporting Information Figure S1). Furthermore, the rates of hydrolysis in three chemically distinct buffers, Hepes, Tris, and phosphate, depended solely on the amount of the 4N complex (Table 4). This indicates that buffer molecules did not participate in the reaction. The exponential (first-order) form of kinetic curves obtained

(22) Hay, R. W.; Hassan, M. M.; You-Quan, C. *J. Inorg. Biochem.* **1993**, *52*, 17–25.
(23) Młynarz, P.; Valensin, G.; Kociołek, K.; Zabrocki, J.; Olejnik, J.; Kozłowski, H. *New J. Chem.* **2002**, *26*, 264–268.
(24) Mylonas, M.; Plakatouras, J. C.; Hadjiliadis, N.; Papavasileiou, K. D.; Melissas, V. S. *J. Inorg. Biochem.* **2005**, *99*, 637–643.

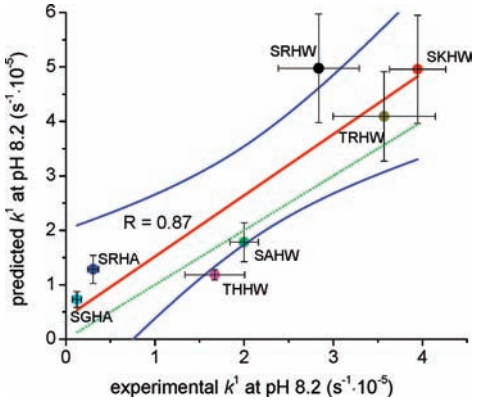

Figure 10. Comparison of actual hydrolysis rate constant values at pH 8.2 and 25 °C (obtained by linear regression of Arrhenius plots, eq 1B) with predicted values, calculated as products of the rate constants at pH 11.6 (100% of 4N complex formation) and relative concentrations of the sum of 4N species at pH 8.2. The trend line (red), 95% confidence bands (blue), and the linear correlation coefficient *R* are marked in the plot. The dotted green line, which marks a theoretical 1:1 correspondence between experimental and predicted rate constants, stays within the limit of 95% prediction bands.

for all peptides under all conditions tested excludes such mechanisms of hydrolysis that would involve two or more Ni(II) complex molecules. Altogether, all these facts confirm an intramolecular character of the reaction mechanism.

The linearity of all Arrhenius plots both at a pH of 8.2 and a pH of 11.6 (Figure 6) and a general similarity of parameters of these plots among the peptides studied indicate that the reaction mechanism is uniform within the temperature and pH range tested. The differences in reactivity among the peptides at a pH of 11.6, while diminished compared to that at a pH of 8.2, remained significant, and the order of reactivity was largely preserved upon the pH increase (Figure 7). These facts indicate that structural factors that govern hydrolysis are different from those providing complex stability. This observation is further illustrated in Supporting Information Figure S4, which compares rate constants at 24 °C (from Supporting Information Tables S1 and S2) with logarithms of $*K_S$ and $*K_P$ (Table 6). The weakness of correlations indicates that neither the stabilities of the Ni(II) complexes of the reaction products nor the ratios of stabilities of Ni(II) complexes of substrates and products affect the rates.

The facts outlined above allowed us to identify the IP structure. First, it must be a product of an intramolecular rearrangement, because its molecular mass was identical with that of the substrate in all cases. Second, the hydrolysis occurs only when a Ser or Thr residue carrying a β-alcoholic group preceded Xaa. Therefore, this alcoholic group is the only possible acceptor of the acyl moiety being removed from the Ser/Thr amide nitrogen atom. The IR spectra of IPs of R_1-SRHW-R_2 and R_1-TRHW-R_2 peptides, but not of their final products or substrates, specifically exhibited a characteristic saturated ester C=O stretch at 1750 cm^{-1}. Taken together, these facts demonstrate that IP is an ester, resulting from the N−O acyl shift to the β-alcoholic group of Ser/Thr. Esters undergo immediate base-catalyzed hydrolysis at high pH but are more stable around neutral pH. This fact is also consistent with an absence of IP at a pH of 11.6 and its presence at a pH of 8.2. The variable IP abundance at the latter pH will

Chart 2. Molecular Mechanism of Ni(II)-Dependent Peptide Hydrolysis of the R_1-Ser/Thr Bond in R_1-(S/T)XHZ-R_2 Peptide Sequences[a]

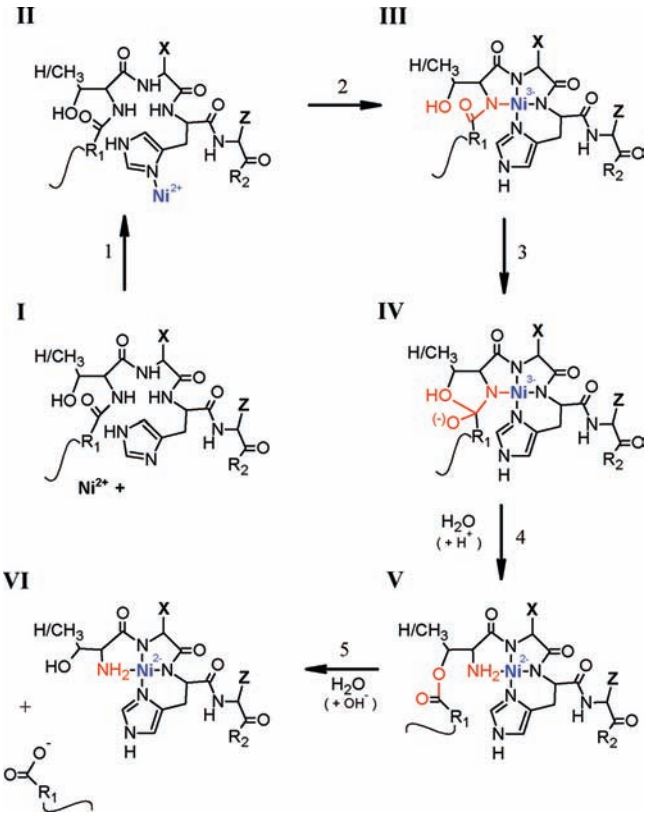

[a] I, apopeptide; II, initial 1N complex with the Ni(II) ion bonded through the imidazole ring; III, stable 4N complex with Ni(II) bonded through the imidazole nitrogen and three preceding amide nitrogens; IV, acyl shift of the R_1 moiety to the Ser/Thr hydroxyl group (a presumable tetrahedral transition state shown); V, intermediate reaction product, containing the ester bonded R_1 moiety; VI, final reaction products: the R_1 peptide, containing a free C-terminal carboxylate, and the Ni(II) complex of the (S/T)XHZ-R_2 peptide.

naturally be due to steric interactions between the R_1 and Xaa moieties.

The requirement of a His two residues downstream from Ser/Thr for the reaction to occur was proved in previous studies.[1−4] This residue acts as an anchor for the Ni(II) ion, enabling the formation of a 4N complex in the middle of the peptide chain.[9,12]

All of these considerations lead to a molecular mechanism of Ni(II)-dependent peptide bond hydrolysis, presented in Chart 2. The process has five steps. It starts with the binding of a Ni^{2+} aqua ion to the peptide, first to the His residue (step 1) and then to three upstream peptide nitrogens (step 2). The 3N species, presented in Chart 1, which contains two Ni(II)-amide bonds, was not shown here, because it is not a hydrolytic species, as discussed above. The formation of a 4N square-planar complex is required for the hydrolysis to occur, as predicted previously and demonstrated hereby.[4,5,10,12,25,26] A high stability of this complex is necessary for the efficient hydrolysis at lower pH values but is less important for

(25) Bal, W.; Djuran, M. I.; Margerum, D. W.; Gray, E. T., Jr.; Mazid, M. A.; Tom, R. T.; Nieboer, E.; Sadler, P. J. *J. Chem. Soc., Chem. Comm* **1994**, 1889–1890.
(26) Bal, W.; Wójcik, J.; Maciejczyk, M.; Grochowski, P.; Kasprzak, K. S. *Chem. Res. Toxicol.* **2000**, *13*, 823–830.

the maximal rate at high pH, where its abundance nears 100% anyway. The planar structure of the complex, imposed by the low-spin Ni(II) ion, bends the peptide chain, placing the nucleophilic Ser/Thr hydroxyl group close to the peptide bond preceding this residue (step 3). The Ni(II) ion destabilizes this peptide bond further by substituting for its hydrogen atom. The sterical mechanism for the acyl shift (step 4) accounts for the results of a statistical analysis of preferred Xaa and Zaa substitutions, presented by us recently.[5] In particular, bulky residues, especially Arg and Lys, which are preferred in position Xaa, provide molecular crowding, which pushes the Ser/Thr hydroxyl group toward the target nitrogen. The methyl group of Thr seems to spoil the productive spatial arrangement a little, and Trp is apparently too large in this position. The full explanation of the positive effect of Trp at position Zaa requires further studies, because the statistical analysis indicated that its effect was lower than predicted by its molecular parameters. The mechanism presented in Chart 2 also accounts very well for the absence of correlation between the stability of the Ni(II) complex and the maximum rate of hydrolysis. The coordination of Ni(II) in the intermediate product is identical to that in the final one. An increase of stability of this 4N complex by several logarithmic units, compared to the substrate (Table 6), is due to the emergence of the amine nitrogen of the Ser/Thr residue. This effect helps prevent the reversal of the acyl shift but has little to do with either the initiation of the acyl shift or with the decomposition of the ester, because these two events do not involve the Ni(II) ion directly. The final step, step 5, of Ni(II)-dependent peptide bond hydrolysis, the intermediate ester product decay, proceeds spontaneously in the presence of water according to the general acid/base catalysis. The data presented in Table 5 indicate, however, that the rates of this decay differ significantly between individual peptides, suggesting secondary interactions, perhaps affecting the availability of the ester bond to the bulk of the solution.

The important role of the Ser or Thr residue in metal-assisted peptide bond hydrolysis was reported previously for a number of dipeptides and related molecules.[27−29] These findings were also interpreted in terms of N−O acyl shift. A similar mechanism was postulated for Cu(II)-related hydrolysis in Ser/Thr−His sequences,[30] and in some Pd(II)/Pt(II)-assisted peptide bond hydrolysis reactions.[31,32] However, in all of these systems, metal ions carried coordinated water molecules, and water activation was considered to be the main role of the metal ion, in an analogy to metalloenzymes. This kind of mechanism is evident, for example, for Pt(II)/Pd(II) hydrolytic reactions with peptides containing no alcoholic residues.[33−39] It was also suggested erroneously for the Ni(II)-dependent reaction in our early paper.[3]

The mechanism demonstrated above and presented in Chart 2 is different, because the first coordination sphere of the square-planar Ni(II) ion is saturated by nitrogen ligands during the reaction. Therefore, the Ni(II) ion cannot activate water molecules directly. Instead, the mechanism presented in Chart 2 resembles the intein mechanism, in which the acyl shift is enabled by a specific distortion of the peptide side chain due to steric hindrance in the protein molecule.[40]

Perspectives of Further Studies. The buffer studies (Table 4) clearly demonstrate that Hepes is the optimal buffer for Ni(II)-dependent hydrolysis at a pH of 8.2 and Tris is slightly inferior, while phosphate is inappropriate. The pH and temperature dependence studies demonstrate that the reaction runs faster at a high pH and high temperature, without compromising its specificity. The experiments discussed above also confirmed the guidelines derived from the library studies about the selection of bulky and hydrophobic amino acids before and after the His residue.[5] These results enable an application of the Ni(II)-dependent peptide bond hydrolysis reaction for recombinant protein engineering.

Conclusions

Previously, we demonstrated that some combinations of Xaa and Zaa substitutions in the general sequence R_1-(Ser/Thr)-Xaa-His-Zaa-R_2 result in peptides which are particularly susceptible to specific hydrolysis of the R_1-(Ser/Thr) peptide bond in the presence of Ni(II) ions. We also found that this particular susceptibility is related to the bulkiness and hydrophobicity of Xaa and Zaa substituents.[5] Hereby, we collected thermodynamic, spectroscopic, and kinetic data, which led to the molecular mechanism of this reaction, on the basis of an intramolecular acyl shift assisted indirectly by the coordinated Ni(II) ion. The optimal reaction conditions include high pH, high temperature, and the absence of competing Ni(II) ligands. These results provide a basis for further development of this reaction for practical applications.

Acknowledgment. This study was financed in part by the Polish Ministry of Science and Higher Education, grant no. PBZ-MIN-007/P04/01 and by the Polish National Center for Research and Development, grant no. KB/138/13749/IT1-B/U/08. We thank Dr. C. Paluszkiewicz of AGH University of Science and Technology, Kraków, Poland for recording the IR spectra.

Supporting Information Available: Full complex species distribution diagrams for R_1-(S/T)XHZ-R_2 peptides and their comparison with UV−vis spectroscopic results, tables of pseudo-first-order rate constants at various temperatures at a pH of 8.2 and 11.6, examples of chromatograms recorded for peptide samples incubated in the presence and absence of Ni(II) ions at pH 11.6, and diagrams of correlations between hydrolysis rate constants at 24 °C and logarithms of stability constants of 4N Ni(II) complexes of R_1-(S/T)XHZ-R_2 and (S/T)XHZ-R_2 peptides. This material is available free of charge via the Internet at http://pubs.acs.org.

(27) Fujii, Y.; Kiss, T.; Gajda, T.; Tan, X. S.; Sato, T.; Nakano, Y.; Hayashi, Y.; Yashiro, M. *J. Biol. Inorg. Chem.* **2002**, *7*, 843–851.
(28) Yashiro, M.; Sonobe, Y.; Yamamura, A.; Takarada, T.; Komiyama, M.; Fujii, Y. *Org. Biomol. Chem.* **2003**, *1*, 629–632.
(29) Yashiro, M.; Yamamura, A.; Takarada, T.; Komiyama, M. *J. Inorg. Biochem.* **1997**, *67*, 225.
(30) Allen, G.; Campbell, R. O. *Int. J. Pept. Protein Res.* **1996**, *48*, 265–273.
(31) Kaminskaia, N. V.; Kostic, N. M. *Inorg. Chem.* **2001**, *40*, 2368–2377.
(32) Manka, S.; Becker, F.; Hohage, O.; Shelderick, W. S. *J. Inorg. Biochem.* **2004**, *98*, 1947–1956.
(33) Milović, N. M.; Kostić, N. M. *J. Am. Chem. Soc.* **2002**, *124*, 4759–4769.
(34) Milović, N. M.; Kostić, N. M. *J. Am. Chem. Soc.* **2003**, *125*, 781–788.
(35) Milović, N. M.; Dutca, L.-M.; Kostić, N. M. *Inorg. Chem.* **2003**, *42*, 4036–4045.
(36) Milović, N. M.; Dutca, L.-M.; Kostić, N. M. *Chem.—Eur. J.* **2003**, *9*, 5097–5106.
(37) Zhu, L.; Kostić, N. M. *Inorg. Chim. Acta* **2002**, *339*, 104–110.
(38) Kaminskaia, N. V.; Johnson, T. W.; Kostic, N. M. *J. Am. Chem. Soc.* **1999**, *121*, 8663–8664.
(39) Kumar, A.; Zhu, X.; Walsh, K.; Prabhakar, R. *Inorg. Chem.* **2010**, *49*, 38–46.
(40) Muir, T. W. *Annu. Rev. Biochem.* **2003**, *72*, 249–289.